J. of Thermal Science Vol.12, No.1

Flow Structure and Heat Transfer Between Two Disks Rotating Independently

Chyi-Yeou Soong
Department of Aeronautical Engineering, Feng Chia University, Seatwen, Taiching, Taiwan 40745 China,
E-mail: cysoong@fcu.edu.tw

In the present paper, fluid flow and convective heat transfer between two co-axial disks rotating independently are dealt with mainly based on the author's recent research on that topic. Three rotational modes, i.e. co-rotation, rotor-stator, and counter-rotation, are considered. Theory of rotating non-isothermal fluids with the presence of disk rotation and thermal effects is addressed. Rotational buoyancy effects on the flow structure development are highlighted. Results of flow visualization and heat transfer measurements are discussed to explore the thermal flow mechanisms involved in the two-disk flows at various rotational and geometric conditions. Potential issues open to the future investigation are also proposed.

Keywords: co-rotating disks, rotor-stator, counter-rotating disks, rotational buoyancy, swirling/vortical flow, heat transfer.

Introduction

Rotating-disk flow is one of the most attractive topics in fluid dynamics. The rotating-disk flow configuration, e.g., two coaxial disks, is simple in geometry but complex in flow physics. With this fact, this class of disk flows can serve as an appropriate model in dealing with the fundamentals of rotating fluids. On the other hand, from the practical point of view, disk configurations have been applied in a number of rotating machinery/devices working with fluids, e.g. rotating heat exchangers, disk-type contactors, rotating-disk-type reactors for metal-organic chemical vapor deposition (MOCVD) of thin film, computer disk storage devices, turbine and compressor disks of turbomachinery etc., in which the thermal-flow behaviors have significant influences on the system performance.

The rotating-disk flow is actually an old topic in fluid dynamics. In 1921, von Karman[1] studied the swirling flow behavior around a disk rotating in quiescent fluids by performing a similarity analysis. Later on, the similarity analysis was extended to deal with the flows between two infinitely large coaxial disks by Batchelor[2] and Stewartson[3]. Two theories proposed distinct descriptions of flow structure for rotor-stator and counter-rotating disks. The controversy between the two theories lasts a long time until the successive works made clarification.

The applications of rotor-stator disks encompass a wide range. Besides that associated with slow rotating devices, e.g. MOCVD reactors and computer disk driver, applications to turbomachinery are of great importance. Lots of efforts have been endeavored towards this area. Owen and Rogers[4] published a monograph to collect the research results of the earlier works (up to 1989) on flow and heat transfer associated with rotor-stator systems. To examine the characteristics of instabilities and the transition process to turbulence in flow between a rotor disk and a stationary casing, Itoh et al.[5] and Schouveiler et al.[6] visualized disk plane view flow patterns and found coexistence of annular and spiral waves at rotational Reynolds number lies in the transitional flow regime. Geis et al.[7] performed the laser-doppler anemometry (LDA) measurements to study flow structure in a double-shrouded rotor-stator cavity with perturbed rotor surface. Recently, Soong et al.[8] conducted an experimental work, by employing heat transfer measurements as well as smoke flow visualization, to study external fluid ingestion into a shrouded rotor-stator system at various conditions. A flow visualization study on flow structure at various conditions is also conducted[9].

In the monograph[4], it is found that only average rather than local heat transfer data were published before

Received 2002

1989. Chyu and Bizzak[10], by using mass-heat transfer analogy based on naphthalene sublimation, examined the effects of radial gap clearance and axial gap spacing on local heat transfer in a shrouded rotor-stator system. Bunker et al.[11,12] used thermochromic liquid crystal technique to measure local heat transfer in a rotor-stator system with hub injection of coolant. Through a narrow tube of 5 mm in diameter at the stator center, a coolant jet at velocity of O (10^2 m/s) impinges onto the center of the rotor surface. Radial distribution of local heat transfer rate shows local heat transfer rate decreases from stagnation point in inboard region (small radius); while in outboard region (large radius) the heat transfer performance is enhanced by the rotational effects. Kim and Kleinman[13] also employed liquid crystal technique to study local heat transfer and cooling effectiveness of a rotor-stator disk system. In their experiments, a coolant jet at velocity around 80 m/s was supplied from an inlet pipe of 7.9 mm in diameter from the stator side. Chen et al.[14] performed both measurements and numerical predictions by an elliptic solver with low-Re $k-\varepsilon$ turbulence model for flow and heat transfer in a shrouded rotor stator system.

By using LDA technique in flow visualization and the flow fields measurements in shrouded co-rotating systems, the phenomenon of the Ekman layer and pumping, the ingress of external fluid[15], inner region of solid-body-like rotation, outer region of large counter-rotating vortices, and a boundary layer region on the shroud[16,17], mean and root-mean-square of the circumferential velocity[18] were studied. Mochizuki and Inoue[19], in their experimental work, addressed self-sustained oscillations in a radial throughflow between open co-rotating disks. With the presence of an axial throughflow, the flow and heat transfer inside heated rotating cavities for a wide range of gap-ratio, rotational Reynolds number, axial Reynolds number were investigated by Fathing et al.[20]. In 1995, Owen and Rogers[21] published another volume of rotating-disk flow and heat transfer with emphasis on rotating cavities. For configuration of computer storage system, numerical predictions for 2-D and 3-D flow structures between a pair of co-rotating disks were performed[22,23] and LDA measurements for vortical flows with/without slide-arm obstruction in a shrouded co-rotating system was carried out[24].

For counter-rotating disks, Dijkstra and van Heijst's[25] numerical results disclosed that a stagnation point appears at the slower-rotating disk as the disks rotate in opposite senses with the rate difference of the two disks above 15%. Duck[26] discussed effects or rotation rates and Reynolds number on the flow patterns and the position of the stagnation point. This stagnation point is associated with a two-cell structure in the cross-sectional view of the gap region. Recently, Gan et al.[27,28] and Kilic et al.[29,30] studied the flow between counter-rotating disks at various ratios of rotating rates of two disks by finite-volume computations of turbulent flow. They concluded that the main effect of a superposed flow is to reduce the core rotation and to promote the flow transition from Batchelor-type to Stewartson-type. Hill and Ball[31,32] presented results of direct numerical simulation of forced convection flow and heat transfer. Their numerical results also found the stagnation point on the slower-rotating disk, which is consistent with the results of Kilic et al.[29]. Gan and Macgregor[33] measured the velocity field in rotor-stator and counter-rotating disk systems without superimposed throughflow and concluded the Batchelor-type flow for the rotor-stator flow and Stewartson-type flow in counter-rotating disk systems. However, among the existing numerical predictions for counter-rotating disks, only that by Soong and Chyuan[34] considered rotational buoyancy effect.

Due to their wide applications in rotating machinery, rotor-stator and co-rotating disks at the same rate have been extensively studied in the past decades. The thermal-flow between disks of counter-rotation received relatively less attention. As to the other rotational conditions, i.e. two disks rotating at different rates in co-rotation or counter-rotation mode, little information of flow and heat transfer exists. Also, due to the difficulties in measurements on rotating-disk systems and the diversity of the possible boundary and operating conditions, study on local heat transfer in rotating disk systems still need more efforts. Additionally, in practical applications of the rotating disk configurations with thermal effects involved, rotation-induced buoyancy effect may be important in certain situations. In the following text, based on some recent studies of the present author, the issues mentioned above are to be addressed and potential topics for the future investigation are also proposed.

Theory of Non-Isothermal Flows Between Rotating-Disks

Most of the earlier works on two-disk flow were concerned with hydrodynamic characteristics only. However, as temperature gradient emerges, the flow field will be inevitably influenced by the thermal effect. In non-isothermal flow, the presence of fluid-temperature gradient and body forces or rotational forces result in thermal buoyancy effects, see Fig.1, which may modify the fluid motion and alter the related heat transfer performance[35]. The rotational buoyancy effect was advocated in an early study of Ostrach and Braum[36]. Either employing compressible flow equations or

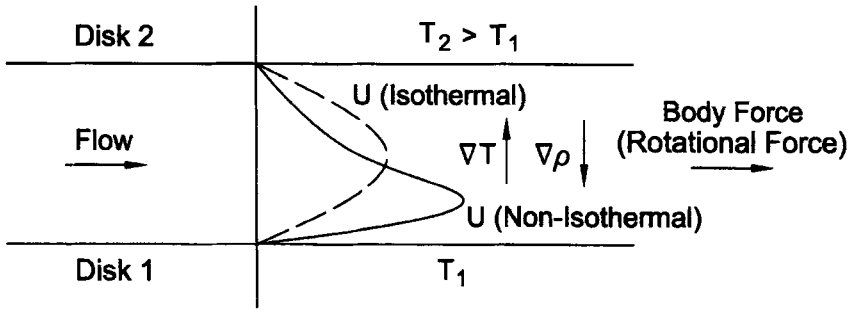

Fig.1 Rotational buoyancy effect in rotating-disk flows

invoking Bousinnesq approximation can model this class of variable-density flow.

For the simplicity in analysis, the Boussinesq fluid model has been extensively employed in the past decades, for example, the theoretical works on infinitely large disks without throughflow in Hudson[37], Chew[38], Soong and Ma[39], Soong[40], Soong and Chyuan[41,42], Soong et al.[43] and the numerical computations for mixed convection between two co-rotating finite disks with effects of radial throughflow and centrifugal buoyancy in Refs.[44, 45].

Navier-Stokes/Boussinesq equations for non-isothermal rotating-disk flows

In this section, equations useful for modeling the non-isothermal rotating disk flows are formulated. Fig.2(a) shows the schematic diagram of two disks rotating independently. A cylindrical rotating frame (R, Z) is fixed on disk 1 and rotating with it. Let the condition of disk 1 be the reference and $\Omega_1 > 0$ in the sense of the rotational speed vector. Positive, zero, and negative values of the rate of the disk 2, Ω_2, stand for the conditions of co-rotation, rotor-stator, and counter-rotation of the system, respectively. The rotational forces exerted on moving fluid particles near the two disks are indicated. It is assumed that the gravitational force and the stress work effects are negligibly small. The flow is assumed laminar with constant properties and Boussinesq approximation is valid. The linear density-temperature relation, $\rho = \rho_r[1-\beta(T-T_r)]$, is employed for accounting the rotational buoyancy effects induced by the body forces. The subscript r denotes the reference condition at disk 1, and the parameter $\beta = -(\partial\rho/\partial T)_P / \rho_r$ is the thermal-expansion coefficient. For the non-body-force terms, the fluid density is regarded as an invariant and expressed as that at reference condition, ρ_r. With the above considerations and approximations, the unsteady form of Navier-Stokes/Boussinesq equations for non-isothermal flow can be formulated as follows:

$$\frac{\partial}{\partial R}(RU)+\frac{\partial V}{\partial \varphi}+\frac{\partial}{\partial Z}(RW)=0 \tag{1}$$

$$\rho_r\left(\frac{\partial U}{\partial t}+U\frac{\partial V}{\partial \varphi}+\frac{V}{R}\frac{\partial U}{\partial \varphi}+W\frac{\partial U}{\partial Z}\right)= \rho_r[1-\beta(T-T_r)]\frac{V^2}{R}-\frac{\partial P_d}{\partial R}- \rho_r\beta(T-T_r)R\Omega_1^2+\rho_r[1-\beta(T-T_r)]2\Omega_1 V+ \mu\left\{\frac{\partial}{\partial R}\left[\frac{1}{R}\frac{\partial(RU)}{\partial R}\right]+\frac{1}{R^2}\frac{\partial^2 U}{\partial \varphi^2}-\frac{2}{R^2}\frac{\partial V}{\partial \varphi}+\frac{\partial^2 U}{\partial Z^2}\right\} \tag{2}$$

$$\rho_r\left(\frac{\partial V}{\partial t}+U\frac{\partial V}{\partial R}+\frac{V}{R}\frac{\partial V}{\partial \varphi}+W\frac{\partial V}{\partial Z}\right)= \rho_r[1-\beta(T-T_r)]\frac{UV}{R}-\frac{1}{R}\frac{\partial P_d}{\partial \varphi}- \rho_r[1-\beta(T-T_r)]2\Omega_1 U+ \mu\left\{\frac{\partial}{\partial R}\left[\frac{1}{R}\frac{\partial(RV)}{\partial R}\right]+\frac{2}{R^2}\frac{\partial^2 U}{\partial \varphi}+\frac{\partial^2 U}{\partial Z^2}\right\} \tag{3}$$

$$\rho_r=\left(\frac{\partial W}{\partial t}+U\frac{\partial W}{\partial R}+\frac{V}{R}\frac{\partial W}{\partial \varphi}+W\frac{\partial W}{\partial Z}\right)=-\frac{\partial P_d}{\partial Z}+ \mu\left[\frac{1}{R}\frac{\partial}{\partial R}\left(R\frac{\partial T}{\partial R}\right)+\frac{1}{R^2}\frac{\partial^2 W}{\partial \varphi^2}+\frac{\partial^2 W}{\partial Z^2}\right] \tag{4}$$

$$\rho_r c_p=\left(\frac{\partial T}{\partial t}+U\frac{\partial T}{\partial R}+\frac{V}{R}\frac{\partial T}{\partial \varphi}+W\frac{\partial T}{\partial Z}\right)= k\left[\frac{1}{R}\frac{\partial}{\partial R}\left(R\frac{\partial T}{\partial R}\right)+\frac{1}{R^2}\frac{\partial^2 W}{\partial \varphi^2}+\frac{\partial^2 W}{\partial Z^2}\right] \tag{5}$$

where $P_d \equiv P - P_r$ is the difference between local pressure and the reference and $\nabla P_r = -\rho_r\Omega_1\times(\Omega_1\times R)$ is the conservative part of the pressure field. Some of the previous studies considered buoyancy effect induced by

the centrifugal forces only, which is referred to as centrifugal-buoyancy (CB) model hereafter. In CB model, only the density variation in the term $-\rho\Omega_1\times(\Omega_1\times R)$ or $R\Omega_1^2$ of the radial momentum equation is considered.

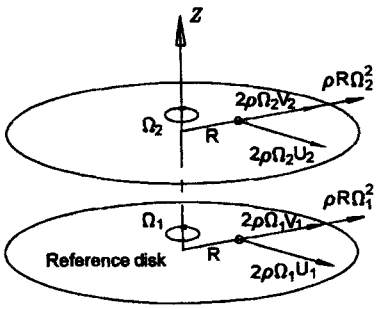

(a) Rotational forces on fluids near disks

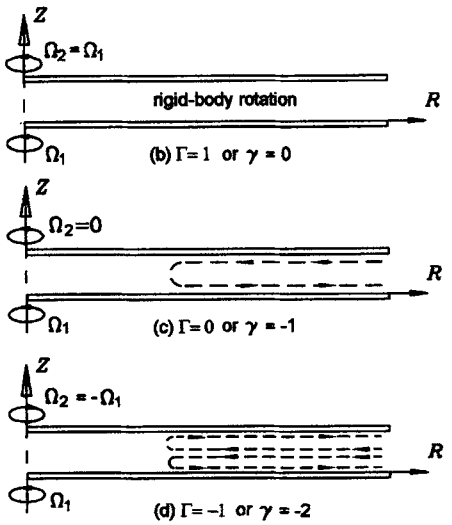

Fig.2 (a) Infinite disks model, coordinates, and the components of rotational force, (b-d) isothermal flow structure of gap-view[9]

Similarity equations for infinitely large disk systems

For exploration of fundamentals of the two-disk flows, assumptions of axisymmetric flow and infinitely large disks can be invoked to facilitate analysis. By using the following dimensionless variables and parameters,

$$\tau=\Omega_1 t,\quad \eta=Z/S,\quad F(\eta,\tau)=U/R\Omega_1$$

$$G(\eta,\tau)=V/R\Omega_1,\quad H(\eta,\tau)=W/(\iota\Omega_1)^{1/2}$$

$$\theta(\eta,\tau)=(T-T_i)/\Delta T_c,\quad Pr=\nu/\alpha$$

$$Re=S^2\Omega_1/\nu,\quad B=\beta\Delta T_c \tag{6}$$

and the definition of characteristic temperature difference defined as $\Delta T_c\equiv T_2-T_1$, the above equations can be cast into either steady-state form [41],

$$H_{\eta\eta\eta\eta}=Re^{1/2}HH_{\eta\eta\eta}+Re^{3/2}[(1+G)G_\eta-B(G_\eta\theta+G\theta_\eta)]-2BRe^{3/2}\theta_\eta-2BRe^{3/2}G(2G\eta\theta+G\theta_\eta \tag{7}$$

$$G_{\eta\eta}=Re^{1/2}[HG_\eta-(1+G)H_\eta+BH_\eta\theta+BGH_\eta\theta] \tag{8}$$

$$\theta_\eta=PrRe^{1/2}H\theta_\eta \tag{9}$$

or, the following time-evolution form [43]:

$$H_{\tau\eta\eta}=Re^{-1}H_{\eta\eta\eta\eta}-4Re^{1/2}(1+G)G_\eta-Re^{1/2}HH_{\eta\eta\eta}+2BRe^{1/2}\theta_\eta+4BRe^{1/2}(\theta G_\eta+G\theta_\eta)+2BRe^{1/2}G(2\theta G_\eta+G\theta_\eta \tag{10}$$

$$G_\tau=Re^{-1}G_{\eta\eta}-Re^{-1/2}(HG_\eta-H_\eta G-H_\eta+B\theta H_\eta+B\theta GH_\eta/2) \tag{11}$$

$$\theta_\tau=(PrRe)^{-1}\theta_{\eta\eta}-\mathrm{Re}^{-1/2}H\theta_\eta \tag{12}$$

For steady flow, the boundary conditions of H, H_η, G, and θ:

$$H(0)=H_\eta(0)=H(1)=H_\eta(1)=0$$
$$G(0)=G(1)-\gamma=0$$
$$\theta(0)=\theta(1)-1=0 \tag{13}$$

are posed on the two disks, where $\gamma\equiv\Omega_2/\Omega_1-1=\Gamma-1$. For time-dependent flow, additional initial conditions need to be prescribed.

The above thermal-flow models were developed based on the Navier-Stokes/Boussinesq equations (1-5) with consideration of all rotational buoyancy effects (RB models for brevity).

Scaling analysis of rotational buoyancy effects

In the previous work[41], the buoyancy effects stemming from each component of body forces were examined in detail. The radial components of body forces consist of the centrifugal and Coriolis forces due to disk rotation, and the centrifugal force due to curvilinear motion of the fluids, viz.,

$$-\rho_r\beta(T-T_r)R\Omega_1^2\sim-\rho_r\beta\Delta T_cR\Omega_1^2 \tag{14}$$

$$-\rho_r\beta(T-T_r)V^2/R\sim-\rho_r\beta\Delta T_cV_c^2/R \tag{15}$$

$$-\rho_r\beta(T-T_r)2\Omega_1V\sim-\rho_r\beta\Delta T_c2\Omega_1V_c \tag{16}$$

Tangential components of buoyancy forces induced by the curvilinear motion of the fluids and the Coriolis force

are, respectively,

$$\rho_r\beta(T-T_r)UV/R \sim \rho_r\beta\Delta T_c U_c V_c/R \quad (17)$$

$$\rho_r\beta(T-T_r)2\Omega_1 U \sim \rho_r\beta\Delta T_c 2\Omega_1 U_c \quad (18)$$

With tangential velocity $V=R(\Omega-\Omega_1)$ in terms of the similarity variable, $G=V/R\Omega_1=(R\Omega-R\Omega_1)/R\Omega_1=(\Omega-\Omega_1)/\Omega_1$, and normalizing the above force components by a reference quantity of centrifugal buoyancy, $\rho_r\beta\Delta T_c R\Omega_1^2$, finally, the order-of-magnitude of the buoyancy components listed in Eqs.(14~18) can be scaled as -1, $-[(\Omega-\Omega_1)/\Omega_1]^2=-G^2$, $-2(\Omega-\Omega_1)/\Omega_1=-2G$, $2/Ro$, and $2[(\Omega-\Omega_1)/\Omega_1]/Ro=2G/Ro$, respectively.

For $\Gamma=1$ (or $\gamma=-1$), Soong[40] proposed a correlation of the Ekman layer thickness, $\delta_E/S=0.782Re^{-1/2}$ with CB model of similarity. Based on the analysis by Soong and Chyuan[41], comparing to the radial centrifugal buoyancy, the order-of-magnitudes of the other radial components are negligibly small. It implies that in the co-rotating disk systems the major contribution to the rotational convection is the centrifugal buoyancy induced by system rotation. On the other words, the CB model is a good approximation for $\Gamma=1$.

As the two disks rotating at different rates and/or in different senses, the rotational forces caused by the two disks become more complicated. In the case of two disks rotate at different rates, even the flow is isothermal, a fluid motion can be driven. Therefore, between two independently rotating disks, the rotation-induced flow is driven by two mechanisms. One is the unbalanced pumping effect in Ekman layers on the two disks; the other is the rotational buoyancy effect. The tangential velocity of the fluid and the local buoyancy effect could be spatially different in the flow field. The buoyancy induced by other components of rotational forces may become important. As the two disks rotating at different rates, therefore, thermal buoyancy effects stemming from all the rotational forces components have to be included in the analysis[41].

Disk rotation-induced buoyancy effects on thermal-flow characteristics

Figs.2(b) ~2(d) display the gap-view of isothermal flow structure. The flow patterns are characterized by solid-body rotation, single-cell, and two-cells for the cases of $\Gamma=1$, 0 and -1 (or $\gamma=0$, -1, and -2), respectively. Fig.3 shows qualitatively the centrifugal buoyancy effects on the flow structures predicted by using CB model[40]. By directly modifying the velocity profiles, the buoyancy has more remarkable influences on the friction factors but relatively weak effects on heat transfer rates[41]. In agreement with the scaling analysis, solutions of similarity models also demonstrate that the rotational buoyancy has little effect on the flow between co-rotating disks at $\Gamma=1$. For two disks rotate independently, the deviations between results of the CB and RB models increase with Reynolds number, *Re*.

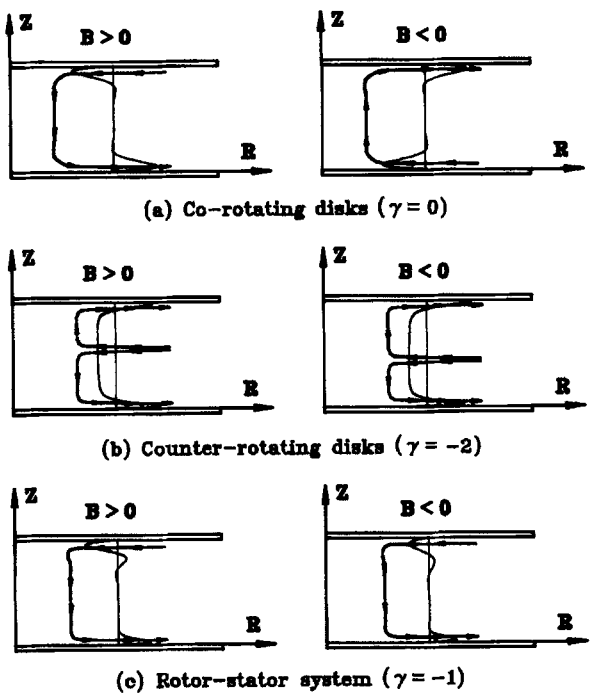

Fig.3 Sketches of gap-view flow structure in infinitely large (a) co-rotating, (b) counter-rotating, and (3) rotor-stator disk systems under influences of centrifugal buoyancy[40]

In a study of disk flow of time-dependence arose from disturbance from one of the disks, the results revealed that the rotational buoyancy affects responses of the flow field[43]. External fluctuations of low frequency and/or high amplitude lead to a larger amplitude of the response oscillation, which can be regarded as a sign of destabilization. Rotating-disk flows at $B<0$ produces a flow field response of relatively larger amplitude than the counterpart cases with $B\le 0$[43]. As for the thermal flow instability in a rotor-stator system, Soong and Tuliszka-Sznitko[46] and the successive works[47, 48] of linear stability analysis disclosed the noticeable effects of thermal Rossby number on the onset condition and the related parameters such as critical wave number, phase speed, wave angle, etc.

In finite disk systems, numerical computations have been used to study the thermal-flow characteristics. For example, Soong and Yan[44,45] studied mixed convection flow and heat transfer between two heated co-rotating disks with consideration of centrifugal buoyancy effect. For flow between a shrouded counter-rotating disk system, Soong and Chyuan's predictions[34] showed the

influence of buoyancy on the thermal flow behaviors, see Fig.4. Although the flow model they used only includes centrifugal buoyancy and more profound and refined calculations need to work on, this preliminary calculations for parametric study still provided clues of the role of buoyancy effect playing in the counter-rotating systems.

In finite disk systems, numerical computations have been used to study the thermal-flow characteristics. For example, Soong and Yan[44,45] studied mixed convection flow and heat transfer between two heated co-rotating disks with consideration of centrifugal buoyancy effect. For flow between a shrouded counter-rotating disk system, Soong and Chyuan's predictions[34] showed the influence of buoyancy on the thermal flow behaviors, see Fig.4. Although the flow model they used only includes centrifugal buoyancy and more profound and refined calculations need to work on, this preliminary calculations for parametric study still provided clues of the role of buoyancy effect playing in the counter-rotating systems.

Experimental Study

An experimental apparatus has been designed and constructed for a series studies on two-disk flow and heat transfer characteristics. Fig.5 shows a schematic diagram with the major components indicated. The experimental apparatus consists of four major parts: (a) coolant air supplier, (b) power section, (c) test section, and (d) measurement and data acquisition system. Each of these subsystems will be described below.

The air was pumped by an air compressor into a tank of 360 liters in volume. Then the air passes through a refrigerated air dryer, which used to cool and dry the air, and then flows through the hollow shaft of the upstream disk. The shaft is of a 40mm inner diameter with a honeycomb as flow straightener into the wheelspace between the disks. The flow rate was measured by a rotary-meter with an accuracy of approximately 3 percent.

Two disks of each test model are driven separately by two three-phase AC electric motors. Each motor is

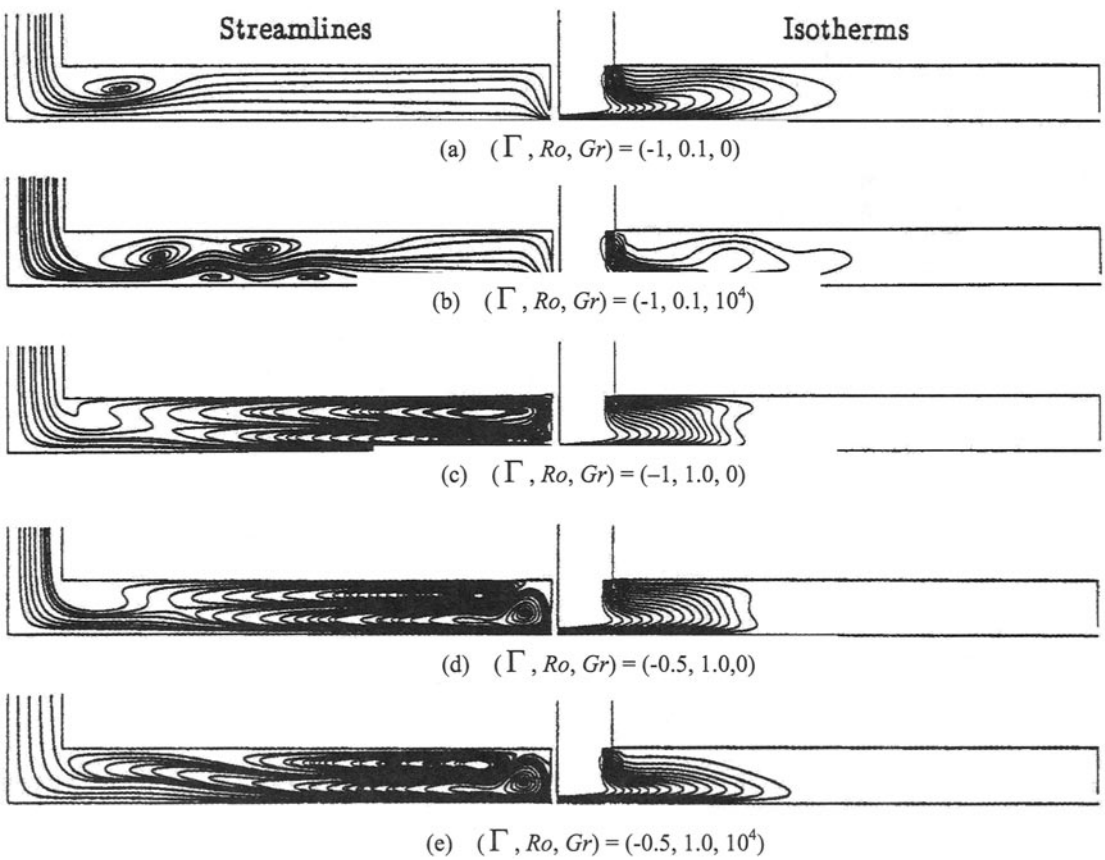

Fig.4 Streamlines and isotherms in a shrouded counter-rotating disk system at

$Re_z = 100, S_c = 0.1.$ $Note: Re_z \equiv W_o S/\nu, Ro \equiv \Omega_1 S/W_o, Gr \equiv (\Omega_1 S)\beta(T_w - T_o)S^3/\nu^2$[34]

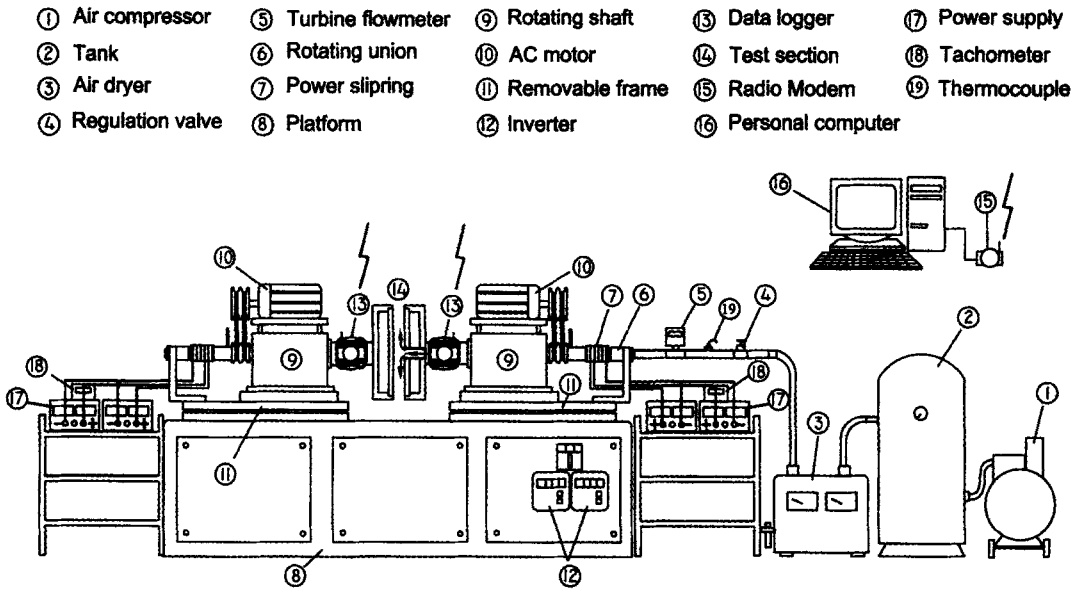

Fig.5 Experimental apparatus for study of thermal-flow between two coaxial disks

equipped with an inverter, by which the rotating rate and sense of the individual disk can be controlled independently. The rotating shaft and supporting bearing system are horizontally mounted on a rigid, heavy steel platform. To detect the rotating rate of each disk, two photoelectric tachometers are installed. The maximum rotating rate of the present rotating disk apparatus is around 2500 rpm. Details of the test sections and instrumentation are described later.

Flow visualization and test models

With minor modification, the experimental apparatus can be used for flow visualization study. An open disk model assembly of radius R_o = 100 mm and a shrouded one of R_o = 150 mm are studied for exploration of fundamental flow mechanisms between coaxially rotating disks with and without the presence of shrouds. For observation and video camera recording one of the two disks in model assembly is made of 10 mm thickness transparent acrylic plate. The tracer for visualizing fluid motion is the paraffin mist from a smoke generator and bleeds slowly into the wheelspace through an opening at a location near the center of one of the disks. To explore the pure rotational effects as well as ensure the quality of the observation, throughflow is not considered. An argon-ion laser beam is turned into a light sheet and employed as the light source for the visualization.

In the most recent work[9], the parameter range encompasses three gap ratios, $G = S/R_o = 0.08$, 0.1, and 0.13; rotational Reynolds number $Re_\Omega = R_o^2\Omega/\nu$ of $O(10^3) \sim O(10^4)$ and the rotating rate ratio $-1.2 \le \Gamma \le 1.2$ are investigated.

Visualization of flow structure between two disks

Fig.6 shows schematic diagrams with characterizing features marked as a summary of the visualization results[9]. It is disclosed that, for open disk systems, co-rotating disk flows are characterized by an inboard core region of solid-body rotation, outboard vortical flow region, and Ekman layers over disks with the presence of the vortex chains in gap-view of the two-cell flow structure. Rotor-stator flow presents annular and/or spiral rolls on rotor disk plane, and Ekman layer on rotor disk in gap flow of single-cell structure. As for the counter-rotating disk systems, the vortical flow structure is of more complexities due to the action of sophisticated rotational forces. Unlike the flow in co-rotating systems, the flow between counter-rotating disks encounters large tangential shear stemming from opposite tangential Coriolis force near two disks. The fluid mixing characteristics are quite good and the premature turbulence can be expected in a disk system of counter-rotation.

From the pictures in Fig.7, it is found that the presence of the shrouds alters the flow structure near the disk rim[8]. The observations further reveal that the symmetric shrouds attached on the disk rim influences the co-rotating disk flow structure mostly. The qualitative nature of the flow structure in a co-rotating shrouded disk system is characterized by the presence of relatively larger vortices near the rim. As to a rotor-stator system, the shroud on disk rim is helpful to the formation of the large-size re-circulation in gap-view. In a counter-rotating system with rim shroud, the strength of the vortex chain is reduced for less external fluid ingested.

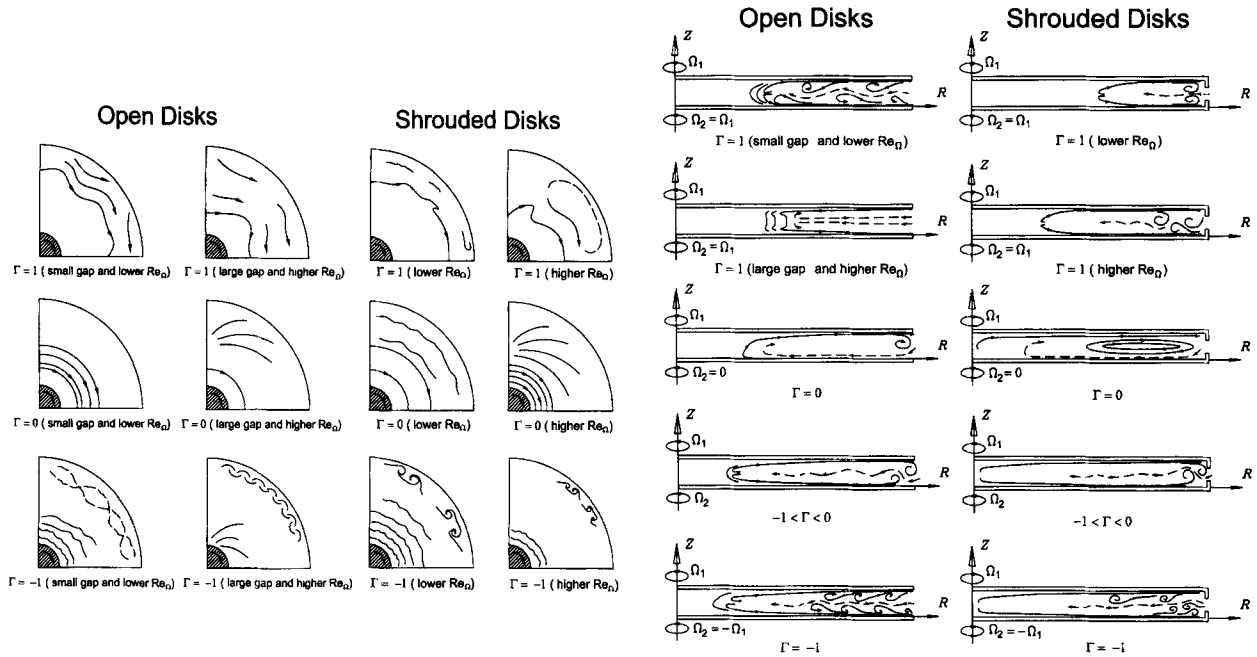

Fig.6 Summary of flow patterns in disk plane-view and gap-view[9]

For counter-rotating disks at different rates, the observations demonstrate the emergence of a stagnation point on the slower-rotating disk in open as well as shrouded systems. The phenomenon is more clearly seen in the disk system with a large gap-ratio. As the rate-ratio Γ varies from –1 to 0, the stagnation point moves radially inward from the rim to the hub and the gap-view flow mode transfers from two-cell to single-cell structure.

These results corroborate some flow natures in co-rotating or rotor-stator systems reported in literature. Meanwhile, relatively novel results of flow visualization between counter-rotating disks and disks rotating at different rates were also disclosed.

External fluid ingestion in rotor-stator systems

In a rotor-stator system, rotor disk tends to pump the fluid radially outward via action of viscous and rotational forces, which accelerates the fluids adjacent to the rotor disk but decelerates the fluids near the stator disk. In the case of fast rotating disk, the fluids pumped out of the wheelspace is more than that provided from the entry coolant flow, the external gas will be ingested along the stator side through the spacing between the clearance at rim. In a practical application of turbomachinery, the external gas flow is a high-temperature gas stream from combustors. The hot gas ingestion is damage to the cooling effectiveness of the turbine disks.

The external fluid ingestion has been studied by visualizing the flow patterns near the rotor-stator disk rim. Under the same throughflow Reynolds number, $Re_z = 2000$, and thermal Rossby number, B=0.034, the flow patterns in Figs.8(a) and 8(b) at $Re_\varphi = 4.3\times10^4$ and 5.9×10^4, respectively, display the ingestion can be promoted by increasing Re_φ. However, with Re_z increased to 3000 in Fig.8(c), the ingestion fluid is purged out. It demonstrates that the enhancement of the forced flow may delay the occurrence of the ingestion. Comparison of Figs.8(c) and 8(d) shows that the higher thermal Rossby number may lead the external fluid ingested into the wheelspace.

Basically, the strong coolant flow can suppress the gas ingress, but the rapid rotation of the rotor disk and the centrifugal buoyancy may induce premature occurrence of the unfavorable ingress phenomena. The flow maps in Figs.8(e) and 8(f) are the summary of the critical condition deduced from the heat transfer measurements and flow visualization results[8].

Heat transfer models and measurements

The heat transfer model of two open disks had an outer radius of 100 mm. The two disks are instrumented with embedded copper-constantan thermocouples (TT-T-30-SLE type) of 0.25 mm diameter for surface temperature measurements. On the casing of each disk, temperature measurements at 7 radial locations are performed and used to estimate convective heat loss from the outer surface of the model assembly. For heat transfer surface temperature measurements, there are 21 thermocouples on the upstream disk and 41 on the

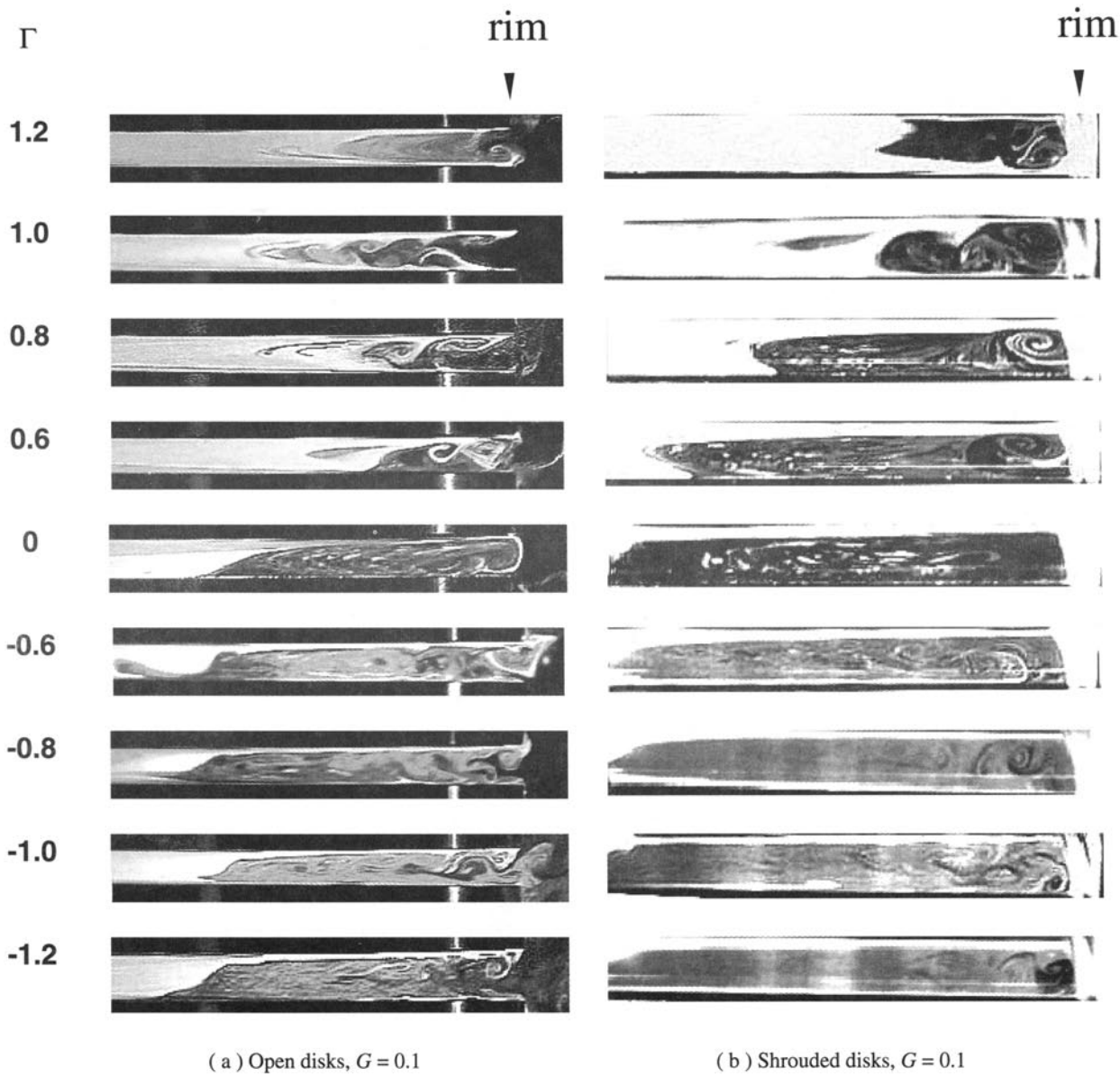

Fig.7 Comparison of gap-view flow structures of open and shrouded disk systems at various rate-ratios[9]

downstream disk including 1 stagnation point at the center of the disk. Two thermocouples are installed on the shaft of each disk, the measurements are used to estimate axial conduction heat loss through the shaft. The inlet temperature of the dried air is measured by a stationary thermocouple located upstream of the inlet of the wheelspace. The bulk fluid temperature, T_b, at each radial location is not measured but estimated based on the principle of thermal energy balance. To check the validity of the estimation, the value of T_b at a location near the exit, i.e. R/R_o = 0.9, is measured by 6 stationary thermocouples at two azimuthal locations 180 degrees apart. The throughflow Reynolds number is fixed as $Re = 10^4$; while the rotating rates of Ω = 500 ~ 2000 r/min and the disk spacing, $G = S/R_o$ = 0.08, 0.1, and 0.13 are considered.

The thermocouple signals on the rotating disks were taken by the ADVANTECH ADAM-4018 slave radio modem modules (accuracy within ±0.1%). Through a wireless transmission to the ADAM-4550 master radio modem module and then through a RS-232 the signals are finally sent to the personal computer for monitoring and controlling of the experiment. In addition, the signals from the stationary thermocouples, e.g. at the exit location, are taken by the YOKOGAWA DA-100 and DS-600 data logger connected to the personal computer.

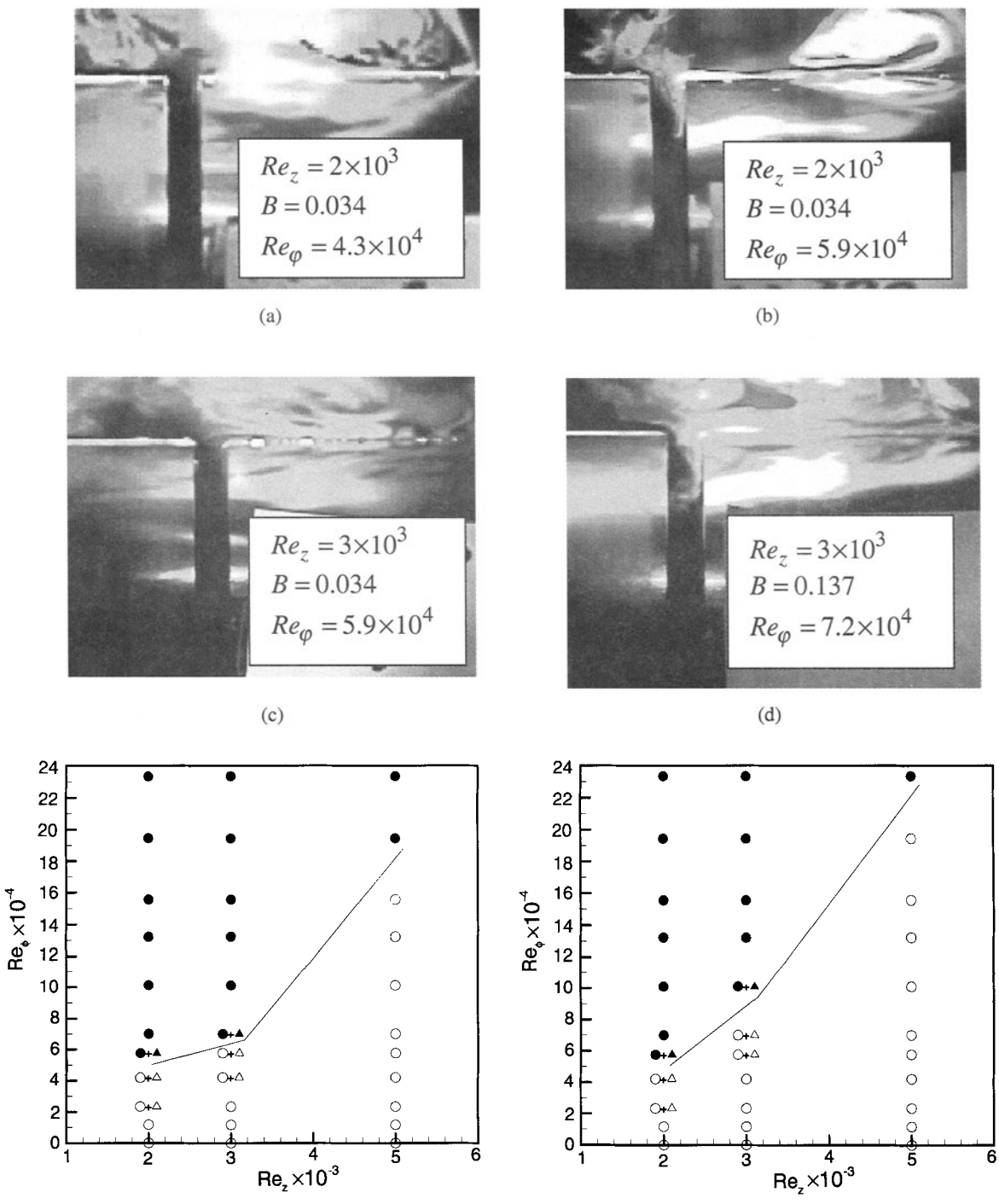

Fig.8 Parametric dependence of occurrence of external fluid ingestion into a shrouded rotor-stator system
(a) and (c): Without ingestion; (b) and (d): with ingestion;
(e) and (f): Flow maps for occurrence of ingestion, in which the solid symbols stand for occurrence of ingestion and the open ones for free of ingestion[8]
(The triangles are translated from heat transfer data)

As all of the surface temperature signals vary within a range of $\pm 0.5°C$ in 3 minutes, the steady state condition is assumed. Typically, it takes about 3 to 4 hrs to reach the steady state for the system starting from idle condition. After that, the test condition is changed to a new one and usually the system reaches the new steady state in a relatively shorter period, e.g. 30 min.

Data reduction and uncertainty analysis

Considering energy balance along the radial direction and heat losses by conduction, convection and radiation, the bulk mean fluid temperature, ΔT_b, and the net heat addition to upstream and downstream disks, $q_{\text{net},u}$ and $q_{\text{net},d}$, can be evaluated. The local heat transfer coefficients, h, and Nusselt number, Nu, on the upstream and downstream disks are determined by the following formulas

$$h_u = q_{net,u}/(T_{w,u} - T_b)\,;$$
$$h_d = q_{net,d}/(T_{w,d} - T_b) \qquad (19)$$

$$Nu_u = h_u R/k = q_{\text{net},u} R/(T_{w,u} - T_b)$$
$$Nu_d = h_d R/k = q_{\text{net},d} R/(T_{w,d} - T_b) \qquad (20)$$

The uncertainty analysis is performed based on the approach for standard single-sample data in Ref. [49]. The uncertainties in axial Reynolds number, rotational Reynolds number are $\pm 3.16\%$, $\pm 2.24\%$, respectively. In the worse case of $Re_z = 10^4$ and the largest rotational Reynolds number, $Re_\varphi = 1.4\times10^5$, the lowest wall-to-coolant temperature difference occurs and the mean wall temperature of the upstream disk was about $58°C$. The uncertainty in local Nusselt number is about 12%.

Measurements of local heat transfer rates

Validation of the measurements. The heat transfer rates in two-disk systems are strongly dependent on local heat flux and wall temperature distributions on both disks. Therefore, even for the same two-disk configuration, it is quite difficult to make comparison between two different experiments in which the heating conditions and the wall-temperature distributions for each are distinct. To verify the experimental and data reduction procedures, theory of a rotating free-disk with a power-law wall-to-ambient temperature difference $\Delta T_c = T_w - T_\infty = cR^n$ [50] is a good reference for comparison. The correlation for the local Nusselt number in transitional and turbulent flow regimes can be obtained,

$$Nu = 0.0197(n+2.6)^{0.2}\,\mathrm{Pr}^{0.6}[Re_\varphi (R/R_o)^2]^{0.8} \qquad (22)$$

The local Nusselt number distribution in radial direction can be calculated with the known values of n and Re_φ (c is a constant but not appears in the Nu-correlation). The correlation, Eq. (22), is usually employed as a reference for verification in experimental works, e.g., in a recent work[51].

Fig.9 shows comparison of the measured local Nusselt numbers[52] with Dorfman's theory at $Re_\varphi = 6.97\times10^4$, 1.04×10^5 and 1.4×10^5, where the first one lies in laminar and the last two in transitional/turbulent flow regimes. It is found that the present data at higher Re_φ in transitional/turbulent flow regime exhibit quite reasonable agreement with the theory; while at low value of $Re_\varphi = 6.97\times10^4$, the data deviate considerably from the theory. The same trend was observed in [51]. The theory without considering natural convection might be the major reason since the

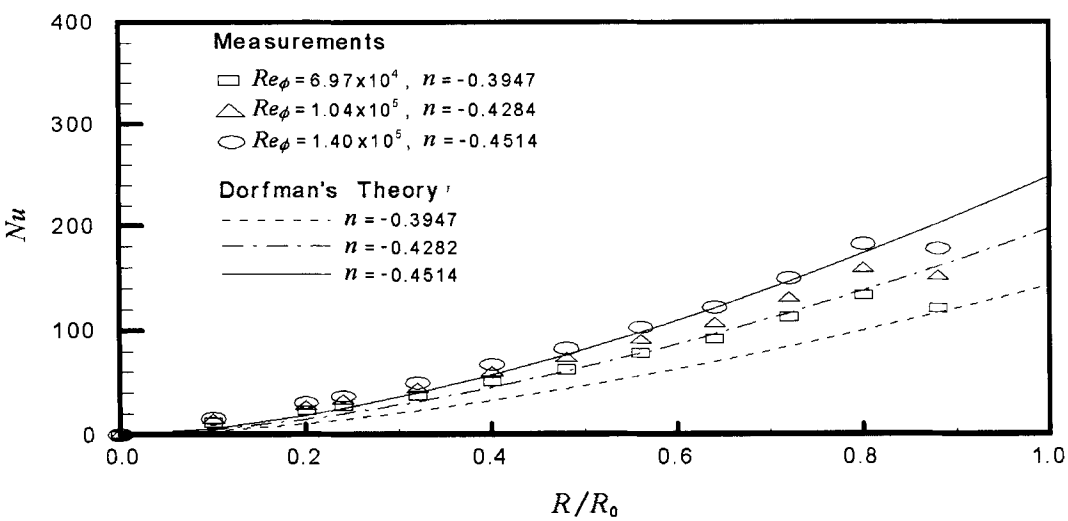

Fig.9 Comparison of the measured local Nusselt numbers[52] with Dorfman's formula from rotating disk theory[50]

buoyancy effects could be significantly influential in a slow rotation case. In outboard region, $0.8 < R/R_o < 1.0$, the discrepancies are attributed to the finite dimension of the disk.

Local heat transfer of rotor-stator system. Fig.10 shows local Nusselt number ratio normalized by a reference quantity for disk at rest. This ratio characterizes heat transfer enhanced by the rotational effects. To explore the influences of the disk rotation on heat transfer, two modes of rotor-stator are considered. Mode A stands for the case of the upstream disk rotating and the downstream disk stationary. While in mode B, the upstream and downstream disks exchange the roles and act as stator and rotor, respectively. It is observed that heat transfer of rotor always better than that on stator. Rotational effects become more noticeable in the outer board region, i.e. $R/R_o > 0.5$. The data for system at gap-ratios G = 0.08 and 0.1 are relatively close to each other and higher than the data at G = 0.133. The closeness of the stator disk influences fluid flow and in turn alters the heat transfer performance.

Local heat transfer of disks with different senses. Fig.11 is a comparison of local heat transfer rate on rotating disk systems of different values of Γ. The data

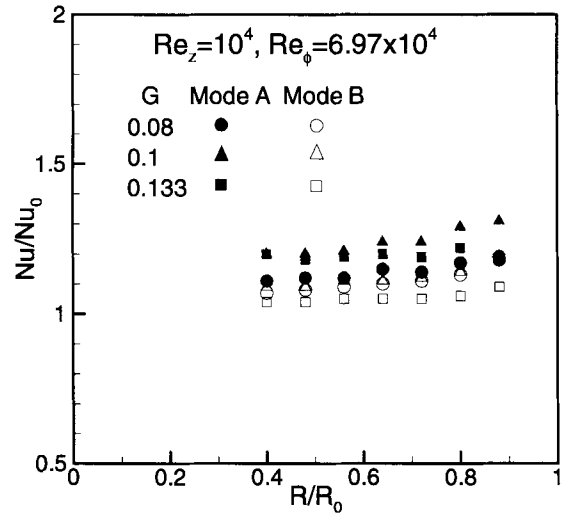

(a) Downstream disk

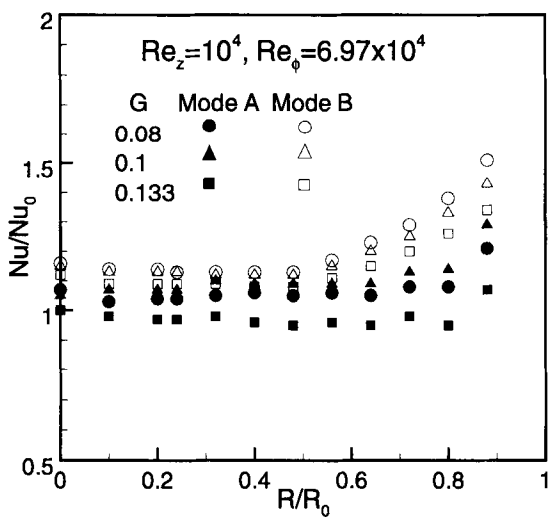

(b) Upstream disk

Fig.10 Local heat transfer on rotor-stator system of mode A: upstream disk rotating and downstream disk at rest, and mode B: downstream disk rotating and upstream disk at rest[52]

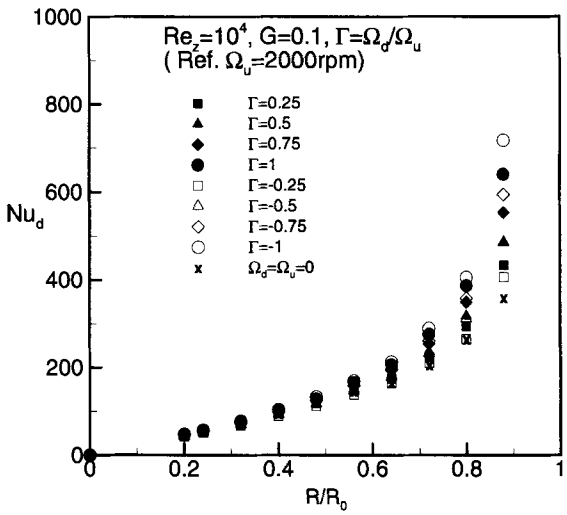

(a) Downstream disk

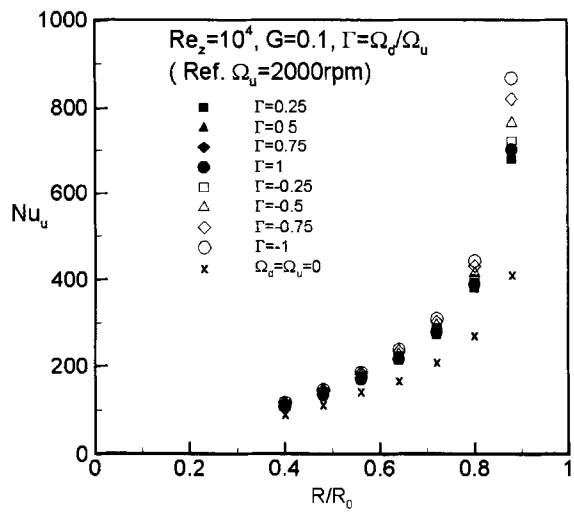

(b) pstream disk

Fig.11 Local heat transfer on a system of two-disks rotating at different rates[53]

for the stationary disks are also displayed. The upstream disk serves as a reference, the downstream disks rotates at various rates ranging from ±500, ±1000, ±1500, ±2000 r/min, i.e. Γ varies from 1 to −1. It is reasonable that the heat transfer increases as the value of $|\Gamma|$ approaching to unity. At the same rates, the counter-rotating disks have slightly higher heat transfer rates than the co-rotating disks.

The better mixing phenomena by the action of the tangential Coriolis force couple in the case of counter-rotating disks could be the major reason.

Concluding Remarks

The present paper has addressed fluid flow and heat transfer characteristics between two coaxial disks rotating at various rate ratios. The recent results of the present author were mainly concerned. Although we have made a lot of efforts on this class of rotating thermal-flow configurations, further investigations are still needed. Some topics worthwhile investigations are proposed as follows:

1. Thermal-flow mechanisms at various rate-ratios need to be further explored. The complexities stem from the interaction and competition of the rotational forces by the two disks are not very clear. Transport phenomena in mixed convection flow and heat transfer with the presence of rotational buoyancy worthwhile to be investigated. The rotational buoyancy assisting and opposing effects on the thermal flow adjacent to the wall could interact with the wall turbulence and the resultant effects must be very distinct from the buoyancy effects in laminar and transitional flows. The details of the coupling nature are not completely understood.

2. So far, only limited works on thermal flow instability in a rotor-stator system under influences of the disk-rotation-induced buoyancy have been conducted. Instability phenomena and mechanisms associated with other rotating-disk configurations at various rotational and thermal conditions are also significant in this field.

3. In an extreme but significant area such as turbo-engine applications, high throughflow Reynolds number, high rotating rate, and high temperature all tends to promote turbulence in the flow field. Numerical simulation of the rotating, non-isothermal, turbulent flow needs reliable turbulence model with inclusion of the rotational buoyancy effects. To develop turbulence model and numerical techniques is significant in improving numerical prediction of rotating non-isothermal flows.

4. For this class of rotating-disk flows with complexities, experimental evidences are always significant and useful in either understanding of the flow physics and development of turbulence model. Development of experimental techniques measurements of high confidence for high rotating rate and/or high temperature systems is most needed.

Acknowledgement

The present work was supported by National Science Council through the grants NSC-89-2212-E-014-006, NSC-89-2212-E-014-015, and NSC-90-2212-E-035-024. My Sincere thanks are also due to Dr. Chang-Chie Wu, Dr. Cheng-Chuang Lai and Dr. Tung-Ping Liu at Rotating Fluids and Vortex Dynamics Laboratory (RFVD Lab), Chung Cheng Institute of Technology for their constant assistance and outstanding performance in the past years.

References

[1] von Karman, Th.. Laminar und Turbulent Reibung. ZAMM, 1921, 1: 233

[2] Batchelor, G K. Note on a Class of Solutions of the Navier-Stokes Equations Representing Steady Rotationally Symmetric Flow. Quart. J. Mech. Applied Math., 1951, 4: 29—41

[3] Stewartson, K. On the Flow Between Two Rotating Coaxial Disks. Proc. Camb. Phil. Soc., 1953, 49: 333—341

[4] Owen, J M, Rogers, R H. Flow and Heat Transfer in Rotating Disc Systems. Rotor Stator Systems, Research Studies Press/John Wiley Inc., New York, 1989, 1

[5] Itoh, M, Yamada, Y, Nagata, H, et al. Characteristics of Instabilities and Transition Processing of the Flow Between a Rotating Disk and the Casing. Trans. Jpn. Soc. Mech. Eng., Ser. B, 1988, 54(502): 1236—1244

[6] Schouveiler, L, Le Gal, P, Chauve, M P. Stability of a Traveling Roll System in a Rotating Disk Flow. Phys. Fluids, 1998, 10(11): 2695—2697

[7] Geis, T, Ebner, J, Kim, S, et al. Flow Structure Inside a Rotor-Stator Cavity. Int. J. Rotating Machinery, 2001, 7(4): 285—300

[8] Soong, C Y, Wu, C C, Liu, T P. Experimental Investigation of External Gas Ingress to a Shrouded Rotor-Stator Disk System. Journal of Chung Cheng Institute of Technology, 2002, 30(2): 99—109

[9] Soong, C Y, Wu, C C, Liu, T P, et al. Flow Structure between Two Coaxial Disks Rotating Independently. Experimental Thermal and Fluid Science, 2002

[10] Chyu, M K, Bizzak, D J. Effects of Axial and Radial-Gap Spacing on the Local Heat Transfer of a Shrouded Rotor-Stator System. ASME J. Heat Transfer, 1992, 114: 1051—1054

[11] Bunker, R S, Metzger, D E, Wittig, S. Local Heat Transfer in Turbine Disk Cavitites: Part I - Rotor and Stator Cooling With Hub Injection of Coolant. ASME J. Turbomachinery, 1992, 114: 211—220

[12] Bunker, R S, Metzger, D E, Wittig, S. Local Heat Transfer in Turbine Disk Cavitites: Part II - Rotor Cooling With Radial Location Injection of Coolant. ASME J. Turbomachinery, 1992, 114: 221—228

[13] Kim, Y W, Kleinman, D A. Heat Transfer and Cooling Effective Studies on Rotating Disks. Heat Transfer in Gas Turbines, HTD-Vol. 300, ASME, 1994, 101—109

[14] Chen, J -X, Gan, X, Owen, J M. Heat Transfer in an Air-Cooled Rotor-Stator System. ASME J. Turbomachinery, 1996, 118: 444—451

[15] Owen, J M, Pincombe, J R. Velocity Measurements Inside a Rotating Cylindrical Cavity with a Radial Outflow of Fluid. J. Fluid Mech., 1980, 99(Part 1): 111—127

[16] Abrahamson, S D, Koga, D J, Eaton, J K. Flow Visualization and Spectral Measurement in a Simulated Rigid Disk Drives. IEEE Trans. on CHMT, 1988, 11(4): 576—584

[17] Abrahamson, S D, Eaton, J K, Koga, D J. The Flow Between Shrouded Corotating Disk. Phys. Fluids A, 1989, 1(2): 241—251

[18] Schuler, C A, Usry, W, Weber, B, et al. On the Flow in the Unobstructed Space Between Shrouded Co-rotating Disks. Phys. Fluids, 1990, 2(10): 1760—1770

[19] Mochizuki, S, Inoue, T. Self-Sustained Flow Oscillations and Heat Transfer in Radial Flow Through Co-Rotating Parallel Disks. Experimental Thermal and Fluid Science, 1990, 3: 242—248

[20] Farthing, P R, Long, C A, Owen, J M, et al. Rotating Cavity with Axial Through Flow of Cooling Air: Flow Structure. ASME J. Turbomachinery, 1992, 114: 237—246

[21] Owen, J M, Rogers, R H. Flow and Heat Transfer in Rotating Disc Systems. Rotating Cavities, Research Studies Press/John Wiley Inc., New York, 1995, 2

[22] Humphrey, J A C, Schuler, C A, Webster, D R. Unsteady Laminar Flow Between a Pair of Disks Corotating in a Fixed Cylindrical Enclosure. Phys. Fluids, 1995, 7(6): 1225—1240

[23] Herrero, J, Giralt, F, Humphrey, J A C. Influence of the Geometry on the Structure of the Flow Between a Pair of Corotating Disks. Phys. Fluids, 1999, 11(1): 88—96

[24] Wu, S J. Flow between Co-Rotating Disks with/without an Obstruction in a Cylindrical Enclosure: [PhD thesis]. Taiwan: Department of Mechanical Engineering, National Taiwan University, 2000

[25] Dijkstra, D, van Heijst, G J F. The Flow between Two Finite Rotating Disks Enclosed by a Cylinder. J. Fluid. Mech., 1983, 128: 123—154

[26] Duck, P W. On the Flow Between Two Rotating Shrouded Discs. Computers and Fluids, 1986, 14(3): 183—196

[27] Gan, X, Kilic, M, Owen, J M. Superposed Flow Between Two Discs Contra-Rotating at Differential Speeds. Int. J. Heat and Fluid Flow, 1994, 15: 438—446

[28] Gan, X, Kilic, M, Owen, J M. Flow Between Contra-Rotating Disks. ASME J. Turbomachinery, 1995, 117: 298—305

[29] Kilic, M, Gan, X, Owen, J M. Transitional Flow Between Contra-Rotating Disks. J. Fluid Mech., 1994, 281: 119—135

[30] Kilic, M, Gan, X, Owen, J M. Turbulence Flow Between Two Disks Contra-rotating at Different Speeds. ASME J. Turbomachinery, 1996, 118: 408—413

[31] Hill, R W, Ball, K S. Chebyshev Collocation Analysis of Axisymmetric Flow and Heat Transfer Between Counter-Rotating Disks. ASME J. Fluids Eng., 1997, 119: 940—947

[32] Hill, R W, Ball, K S. Direct Numerical Simulations of Turbulent Forced Convection Between Counter-Rotating Disks. Int. J. Heat Fluid Flow, 1999, 20: 208—221

[33] Gan, X P, Macgregor, S A. Experimental Study of the Flow in the Cavity Between Rotating Disks. Experimental Thermal and Fluid Science, 1995, 10: 379—387

[34] Soong, C Y, Chyuan, C H. Navier-Stokes Computations of Non-Isothermal Flow and Heat Transfer Between Counter-Rotating Disks. Edited by D.C. Han et al. Proceedings of the 6th International Symposium on Transport Phenomena and Dynamics of Rotating Machinery, 1996, 2: 39—46

[35] Soong, C Y. Thermal Buoyancy Effects in Rotating Non-Isothermal Flows. Int. J. Rotating Machinery, 2001, 7(6): 435—446

[36] Ostrach, S, Braum, W H. Natural Convection Inside a Flat Rotating Container. NACA TN 4323, 1958

[37] Hudson, J L. Non-Isothermal Flow between Rotating Disks. Chem. Eng. Sci., 1968, 23: 1007—1020

[38] Chew, J W. Similarity Solutions for Non-Isothermal Flow Between Infinite Rotating Disks: [Report TFMRC/38]. UK: Thermo-Fluid Mech. Res. Centre, School Eng. Appl. Sci, University of Sussex, 1981

[39] Soong, C Y, Ma, H L. Unsteady Analysis of Non-Isothermal Flow and Heat Transfer Between Rotating Co-axial Disks. Int. J. Heat Mass Transfer, 1995, 38(10): 1865—1878

[40] Soong, C Y. Theoretical Analysis for Axisymmetric Mixed Convection Between Rotating Coaxial Disks. Int. J. Heat Mass Transfer, 1996, 39(8): 1569—1583

[41] Soong, C Y, Chyuan, C H. Investigation of Buoyancy Effects in Non-Isothermal Rotating Flows by Scaling Analysis and a Novel Similarity Model. The Chinese Journal of Mechanics, 1998, 14(4): 193—207

[42] Soong, C Y, Chyuan, C H. Similarity Solutions of Mixed Convection Heat Transfer in Combined Stagnation and Rotating-Induced Flows over a Rotating Disk. Heat and Mass Transfer, 1998, 34(2-3): 171—180

[43] Soong, C Y, Liu, T P, Wu, C C. Dynamical Response of Non-Isothermal Flow between Two Independently Rotating Disks with Time Dependent Wall Conditions. Heat and Mass Transfer, 2002

[44] Soong, C Y, Yan, W M. Numerical Study of Mixed Convection Between Two Co-Rotating Symmetrically Heated Disks. AIAA J. Thermophysics Heat Transfer, 1993, 7(1): 165—170

[45] Soong, C Y, Yan, W M. Transport Phenomena in Non-Isothermal Flow Between Co-rotating Asymmetrically-Heated Disks. Int. J. Heat Mass Transfer, 1994, 37(15): 2221—2230

[46] Soong, C Y, Tuliszka-Sznitko, E. Linear Stability Analysis of Rotation-Induced Mixed Convection in a Rotor-Stator Disk System. Proc. of the 8th International Symposium of Transport and Dynamics of Rotating Machinery (ISROMAC-8), Honolulu, Hawaii, USA, 2000

[47] Tuliszka-Sznitko, E, Soong, C Y. Instability of Non-Isothermal Flow Between Coaxial Rotating Disks. European Congress on Computational Methods in Applied Sciences and Engineering (ECCOMAS 2000), Barcelona, Spain, 2000

[48] Tuliszka-Sznitko, E, Soong, C Y, Serre, E, et al. Absolute Instability of the Non-Isothermal Flow Between Coaxial Rotating Disks. European Congress on Computational Methods in Applied Sciences and Engineering (ECCOMAS 2001), Swansea, Wales, UK, 2001

[49] Kline, S J, McClintock, F A. Describing Uncertainties in Single Sample Experiments. Mechanical Engineering, 1953, 3—8

[50] Dorfman, L A. Hydrodynamic Resistance and the Heat Loss of Rotating Solid. Translated by N. Kemmer, Oliver & Boyd, Edinburgh and London, UK, 1963

[51] Northrop, A, Owen, J M. Heat Transfer Measurements in Rotating-Disc Systems Part 1: The Free Disc. Int. J. Heat Fluid Flow, 1988, 9(1): 19—26

[52] Soong, C Y, Liu, T P, Lai, C C, et al. Local Heat Transfer Characteristics in a Rotor-Stator Disk System at Various Rotational Conditions. Submitted for Publication, 2002

[53] Soong, C Y, Liu, T P, Lai, C C. Experimental Investigation of Local Heat Transfer Between Two Coaxial Disks Rotating at Various Rate Ratios. Submitted for Publication, 2002